



HAL
open science

Loter: A software package to infer local ancestry for a wide range of species

Thomas Dias-Alves, Julien Mairal, Michael Blum

► **To cite this version:**

Thomas Dias-Alves, Julien Mairal, Michael Blum. Loter: A software package to infer local ancestry for a wide range of species. 2017. hal-01630228v1

HAL Id: hal-01630228

<https://inria.hal.science/hal-01630228v1>

Preprint submitted on 7 Nov 2017 (v1), last revised 27 Aug 2018 (v3)

HAL is a multi-disciplinary open access archive for the deposit and dissemination of scientific research documents, whether they are published or not. The documents may come from teaching and research institutions in France or abroad, or from public or private research centers.

L'archive ouverte pluridisciplinaire **HAL**, est destinée au dépôt et à la diffusion de documents scientifiques de niveau recherche, publiés ou non, émanant des établissements d'enseignement et de recherche français ou étrangers, des laboratoires publics ou privés.

1 Loter: A software package to infer local ancestry for a wide range
2 of species

3 Thomas Dias-Alves,¹ Julien Mairal,² Michael G.B. Blum,^{*,1}

4
5 ¹ Univ. Grenoble Alpes, CNRS, Grenoble INP*, TIMC-IMAG UMR 5525, Grenoble, France

6 ² Univ. Grenoble Alpes, Inria, CNRS, Grenoble INP*, LJK, 38000 Grenoble

7
8 Running Head: Loter: A software package to infer local ancestry

9 Keywords: Corresponding author: Michael Blum

10 Laboratoire TIMC-IMAG, Faculté de Médecine, 38706 La Tronche, France

11 Phone +33 4 56 52 00 65

12 Email: michael.blum@univ-grenoble-alpes.fr

Abstract

Admixture between populations provides opportunity to study biological adaptation and phenotypic variation. Admixture studies can rely on local ancestry inference for admixed individuals, which consists of computing at each locus the number of copies that originate from ancestral source populations. Existing software packages for local ancestry inference are tuned to provide accurate results on human data and recent admixture events. Here, we introduce Loter, an open-source software package that does not require any biological parameter besides haplotype data in order to make local ancestry inference available for a wide range of species. Using simulations, we compare the performance of Loter to HAPMIX, LAMP-LD, and RFMix. HAPMIX is the only software severely impacted by imperfect haplotype reconstruction. Loter is the less impacted software by increasing admixture time when considering simulated and admixed human genotypes. LAMP-LD and RFMIX are the most accurate method when admixture took place 20 generations ago or less; Loter accuracy is comparable or better than RFMix accuracy when admixture took place of 50 or more generations; and its accuracy is the largest when admixture is more ancient than 150 generations. For simulations of admixed *Populus* genotypes, Loter and LAMP-LD are robust to increasing admixture times by contrast to RFMix. When comparing length of reconstructed and true ancestry tracts, Loter and LAMP-LD provide results whose accuracy is again more robust than RFMix to increasing admixture times. We apply Loter to admixed *Populus* individuals and lengths of ancestry tracts indicate that admixture took place around 100 generations ago.

31 Introduction

32 Admixture or hybridization between populations is a natural phenomenon that provides opportunity to map genomic
33 regions involved in phenotypic variation and biological adaptation (Buerkle and Lexer 2008; Payseur and Rieseberg
34 2016). Mapping can rely on Local Ancestry Inference (LAI) of admixed individuals, which consists of computing at
35 a given locus the number of copies that originates from the ancestral source populations. LAI makes use of haplo-
36 types from putative source populations and processes haplotypes or genotypes from admixed population to infer local
37 ancestry of admixed individuals. Figure 1 shows local ancestry of four simulated *Populus* individuals resulting from
38 admixture between two *Populus* species (Suarez-Gonzalez et al. 2016). Sequence and dense genotype data are now
39 generated for a wide range of species besides humans for which LAI is relevant. LAI can be used to study patterns
40 of introgression (Hufford et al. 2013; Suarez-Gonzalez et al. 2016; Medugorac et al. 2017), to map genes involved
41 in reproductive isolation (Corbett-Detig and Nielsen 2017) and phenotypic variation (Lindtke et al. 2013; vonHoldt
42 et al. 2016), and to decipher past admixture processes (Brandvain et al. 2014; Liu et al. 2014). Although various LAI
43 software have been developed, they have been mainly tuned to human data in order to map disease-associated variants
44 (Patterson et al. 2004; Seldin et al. 2011).

45 In this paper, we introduce the software package Loter for Local Ancestry Inference, which does not require spec-
46 ifications of statistical or biological parameters in order to make LAI available for a wide range of species. Several
47 software packages for LAI have been developed including HAPMIX, LAMP-LD, and RFMIX (Price et al. 2009; Baran
48 et al. 2012; Maples et al. 2013). However, they require various parameters to be specified, which can hamper their prac-
49 tical use. HAPMIX requires specifications of several biological parameters that might be difficult to obtain such as
50 genetic maps, recombination and mutation rate, average ancestry coefficients, and the average number of generations
51 since admixture (Price et al. 2009). LAMP-LD requires a physical map and statistical parameters such as the num-
52 ber of hidden states in the hidden Markov Model and a window size where local ancestry is assumed to be constant
53 (Baran et al. 2012). Default parameter values can be provided when using LAMP-LD. RFMIX requires statistical
54 and biological parameters, which are a genetic map, a window size (in centimorgan) where local ancestry is assumed
55 to be constant, and the average number of generations since admixture (Maples et al. 2013). Except for the genetic
56 map, default parameters values can also be provided when using RFMIX (Maples et al. 2013). Other less-important
57 differences between LAI software packages are also provided in Table 1. Except for LAMP-LD that uses statistical
58 parameters only, RFMIX and HAPMIX require biological information such as genetic map, which can be difficult to
59 provide for non-model species.

60 The software package Loter is based on the copying model introduced by Li and Stephens (2003) and already used
61 in HAPMIX to perform LAI (Price et al. 2009). The copying model assumes that given a collection of “parental”
62 haplotypes from putative source populations, haplotypes from admixed individuals are modeled as a mosaic of exist-

ing parental haplotypes (Figure 2). The main difference with HAPMIX is that Loter is not based on a probabilistic formulation, which requires several parameters to be specified. Instead, Loter is based on an optimization problem parametrized with a single regularization value λ that penalizes switches between parental haplotypes. Solutions of the optimization problem are found by using a dynamic programming algorithm, whose computational complexity is linear with respect to the number of markers and the number of individuals from the source populations. Inference of local ancestry is found by averaging results obtained for different values of the regularization parameter λ and various runs of the algorithm.

We compare Loter to HAPMIX, LAMP-LD and RFMIX using diploid accuracy, which is an error measure analogous to imputation error for LAI (Sankararaman et al. 2008). We consider an admixture experiment using human genotypes from HAPMAP 3 where we simulate genotypes resulting from admixture between Europeans (CEU) and Africans (YRI) (International HapMap 3 Consortium et al. 2010). We evaluate to what extent diploid accuracy is affected by the number of generations since admixture for the different approaches. We additionally consider a 3-way admixture scenario between Chinese (CHB), Europeans (CEU) and Africans (YRI) from HAPMAP 3. We repeat admixture simulations using genotypes from two *Populus* species in North America (Figure 1) (Suarez-Gonzalez et al. 2016). We additionally evaluate to what extent length of ancestry tracts are accurately inferred by the different LAI software packages. Length of ancestry tracts is a biological information that is used to date and reconstruct admixture events and that should consequently be accurately inferred for reliable demographic reconstruction (Gravel 2012; Ni et al. 2016; Corbett-Detig and Nielsen 2017; Xue et al. 2017). Finally, we apply Loter to admixed *Populus* genotypes, and we estimate admixture time using length of reconstructed ancestry tracts.

New Approaches

We describe the optimization problem, which accounts that haplotypes from admixed individuals are described as a mosaic of haplotypes originating from the source populations (Figure 2). We assume that there are n individuals in the source populations resulting in $2n$ haplotypes denoted by (H_1, \dots, H_{2n}) . The value (0 or 1) of the i^{th} haplotype at the j^{th} SNP is denoted by H_i^j . Haplotypes can be obtained from genotypes using computational phasing software such as fastPHASE or Beagle (Scheet and Stephens 2006; Browning and Browning 2007). A vector (s_1, \dots, s_p) describes the sequence of haplotype labels from which the haplotype h of an admixed individual can be approximated (Figure 2). For the j^{th} SNP in the data set, $s_j = k$ if haplotype h results from a copy of haplotype H_k . The optimization problem consists of minimizing the following cost function

$$C(s_1, \dots, s_p) = \sum_{j=1}^p |h^j - H_{s_j}^j| + \lambda \sum_{j=1}^{p-1} \mathbb{1}_{s_j \neq s_{j+1}}, \quad (1)$$

91 where (s_1, \dots, s_p) is in $\{1, \dots, 2n\}^p$. The first term in equation (1) is a loss function that sums over all possible
92 loci of a $\{0, 1\}$ -valued function equals to 1 if haplotype h is different from the copied haplotype and to 0 otherwise.
93 The second term is a regularization term that is equal to the regularization parameter λ times the number of switches
94 between parental haplotypes. A solution to minimize equation (1) can be found using dynamic programming and is
95 provided in the Materials and Methods section. Once a solution has been provided about the sequence (s_1, \dots, s_p)
96 of parental haplotypes, local ancestry values can be deduced automatically from this sequence because each parental
97 haplotype belongs to one of the source populations (Figure 2). The formulation described in equation (1) is valid for
98 $K = 2$ or more ancestral source populations.

99 The optimization problem described in equation (1) involves a regularization parameter λ . Large values of λ
100 strongly penalize switches between parental haplotypes such that solutions have long chunks of constant local ancestry.
101 To avoid the difficult choice of λ , solutions for local ancestry are averaged by running the optimization method several
102 times on different values of λ . Besides, to improve the stability of the solution, for each value of λ , we consider a
103 bagging technique where 20 different solutions are found based on 20 different datasets generated using bootstrap with
104 resampling (Breiman 1996). We consider $\lambda = 1.5, 2, 2.5, 3, 3.5, 4, 4.5, 5$ resulting in $160 = 8 \times 20$ different solutions
105 and the final choice for local ancestry is obtained using a majority rule. When the most frequent vote has less than 75%
106 of the votes, ancestry is imputed using local ancestry values of the closest SNPs with a preference for the SNP on the
107 left in case of ambiguity. Finally, an additional smoothing procedure is considered in order to account for switch errors
108 when phasing admixed individuals (see Materials and Methods).

109 **Results**

110 **Simulated human admixed individuals**

111 We consider simulated admixed individuals resulting from admixture between Africans (YRI population in HAPMAP
112 3) and Europeans (CEU population in HAPMAP 3). Accuracy obtained with several LAI software packages varies
113 depending on time since admixture occurs (Figure 3). For recent admixture where admixture occurred 5 generations
114 ago, LAMP-LD and RFMix obtain the best result with median diploid accuracies of 99.6% and 99.8% whereas median
115 diploid accuracy of Loter is equal to 99.3%. For ancient admixture where admixture occurred 500 generations ago,
116 Loter obtains the largest median diploid accuracy of 86.7% followed by LAMP-LD with a diploid accuracy of 80.6%
117 and RFMix with a diploid accuracy of 72.0%. For the smallest admixture times ($\mu \leq 20$ generations), diploid accuracy
118 obtained with the three approaches is larger than 95% and RFMix and LAMP-LD outperform LOTER. By contrast, for
119 the largest admixture times ($\mu \geq 150$ generations), Loter is the most accurate software for LAI (Figure 3).

120 We evaluate the benefit of bagging and of averaging local ancestry values obtained with different values of the

121 regularization parameter, which are implemented by default in Loter. First, diploid accuracy depends on the choice of
122 the regularization parameter (Supplementary Figure S11). As expected, smallest values of λ provide the best result for
123 ancient admixture event; $\lambda = 2$ is optimal when $\mu = 400$ and $\mu = 500$ generations, and $\lambda = 5$ is optimal otherwise.
124 Second, for all values of the admixture times, averaging local ancestry values obtained with different values of the
125 regularization parameter λ instead of considering a single value improves inference (Supplementary Figure S11). Last,
126 averaging over bootstrap replicates (bagging) further improves local ancestry inference (Supplementary Figure S11).

127 We additionally evaluate the diploid accuracy of HAPMIX, which is another LAI software package based on the
128 copying model. Compared to the three other LAI software packages, its diploid accuracy is the smallest with values
129 of diploid accuracy ranging from 42% to 57% (Supplementary Figure S12). The fact that haplotypes used for LAI are
130 not exact but can be computationally phased using Beagle causes the severe reduction of diploid accuracy obtained
131 with HAPMIX (Supplementary Figure S13). When considering haplotypes reconstructed with Beagle instead of true
132 haplotypes, diploid accuracy is reduced by 32% in average.

133 Additionally, we compare diploid accuracy of Loter, RFMix and LAMP-LD on data simulated under a 3-way
134 admixture model (Supplementary Figure S14). As for 2-way admixture model, we find that RFMix and LAMP-LD
135 have larger diploid accuracies than Loter for recent admixture and smaller ones for ancient admixture. When admixture
136 took place 5 generations ago, the diploid accuracy of RFMix is of 99.8%, the accuracy of LAMP-LD is of 99.8%, and
137 the accuracy of Loter is of 99.5%. By contrast, when admixture took place 500 generations ago, the diploid accuracy
138 of RFMix is of 84.6%, the accuracy of LAMP-LD is of 89.1%, and the accuracy of Loter is of 92.3%.

139 **Simulated *Populus* admixed individuals**

140 We simulate individuals that result from admixture between *Populus trichocarpa*, which is adapted to relatively humid,
141 moist, and mild conditions west of the Rocky Mountains and *Populus balsamifera*, which is a boreal species (Suarez-
142 Gonzalez et al. 2016). As for human data, we compare Loter, RFMix, and LAMP-LD using diploid accuracy as a
143 criterion for comparison. Again, the diploid accuracy of RFMix decreases with increasing admixture time. It ranges
144 from a diploid accuracy of 92.0% when admixture occurs 5 generations ago to a diploid accuracy of 65.3% when
145 admixture occurs 500 generations. By contrast to the simulations of human data, we find that the diploid accuracy of
146 Loter and of LAMP-LD does not change with admixture time. For LAMP-LD, diploid accuracies ranges from 91.3%
147 to 90.1% and for Loter it ranges from 89.9% to 89.0% when admixture increases from 5 to 500 generations.

148 **Length of ancestry tracts**

149 For simulated admixed *Populus* individuals, we additionally compare the length of *P. balsamifera* reconstructed an-
150 cestry tracts to the length of true ancestry tracts (Figure 5). When admixture took place 10 generations ago, RFMIX

151 provides a distribution of ancestry tracts that is closer to the true distribution. For *Populus* simulations, the true median
152 length of ancestry tract is of 4.26 cM and RFMIX finds 5.20 cM whereas LAMP-LD and Loter find median lengths of
153 0.05 and 2.31 cM respectively. Both LAMP-LD and Loter return spurious chunks of local ancestry of small lengths
154 and that contribute to reduce the mean length of local ancestry (Supplementary Figure SI6). Additionally, several long
155 blocks of ancestry chunks are cut into smaller pieces when using Loter or LAMP-LD (Supplementary Figure SI6).
156 When admixture took place 10 generations ago in the human simulations, both Loter and RFMIX provide the most
157 accurate results; the true median length of ancestry tract is of 9.03 cM and RFMIX, Loter, and LAMP-LD reconstruct
158 ancestry tracts of median length 9.99 cM, 12.20 cM and 9.02 cM, respectively.

159 When admixture took place 200 or of 500 generations, length of ancestry chunks are more accurately reconstructed
160 with Loter and with LAMP-LD than with RFMIX (Figure 5). For both human and *Populus* simulated data, RFMIX,
161 by contrast to Loter and LAMP-LD, reconstructs ancestry tracts that are too long compared to true ancestry tracts
162 when admixture is larger or equal than 200 generations. When admixture took place 200 generations ago, true median
163 ancestry tracts is of 1 cM or less whereas RFMIX reconstructs tracts of 2 cM or more. For *Populus* simulations, the true
164 median length of ancestry tract is of 0.45 cM when admixture took place 200 generations ago, and RFMIX, Loter, and
165 LAMP-LD find respectively 2.00 cM, 0.56 cM and 0.30 cM (Supplementary Figure SI6). When admixture took place
166 500 generations ago, the true median length of ancestry tract is of 0.17 cM, and RFMIX, Loter, and LAMP-LD find
167 respectively 1.60 cM, 0.33 cM and 0.17 cM.

168 **Application of Loter to admixed *Populus* individuals**

169 We applied Loter to 36 individuals that are admixed between *P. balsamifera* and *P. trichocarpa*. When averaging local
170 ancestry coefficients, we find that admixed individuals have on average 87% of *P. trichocarpa* ancestry and 13% of *P.*
171 *balsamifera* ancestry. We find that the median length of *P. balsamifera* ancestry tracts is equal to 0.76 cM and the first
172 and third quartiles are equal to 0.25 cM and 1.47 cM. We also perform simulations of admixed individuals based on true
173 genotypes from *P. balsamifera* and *trichocarpa* individuals. When admixture time varies from 10 to 500 generations;
174 median reconstructed *P. balsamifera* ancestry tracts vary from 2.3 cM to 0.32 cM, the first quartile varies from 0.28
175 cM to 0.19 cM, and the third quartile varies from 4.18 cM to 0.55 cM (Figure 6). Of the six admixture times we
176 considered ($\mu \in \{10, 50, 100, 200, 300, 500\}$) in the simulations, we find that $\mu = 100$ generations provide the most
177 similar distribution of *P. balsamifera* ancestry tracts; when $\mu = 100$ generations, the three quartiles of *P. balsamifera*
178 ancestry tracts are equal to 0.21 cM, 0.78 cM, and 1.29 cM.

179 Discussion

180 As dense genotype or sequencing data become more affordable, local ancestry inference provides an opportunity for
181 admixture mapping and for deciphering admixture processes as well. We have introduced the software package Loter
182 in order to make local ancestry available for a wide range of species for which biological parameters such as admixture
183 times or recombination rates are not available. The regularization parameter λ , which controls smoothing, depends in
184 a complicated manner on several biological and statistical parameters including mutation and recombination rates. To
185 avoid the difficult choice of the regularization parameter, Loter implements an averaging procedure where we average
186 solutions for different values of the regularization parameter. Because of an appropriate model averaging strategy,
187 Loter is robust to the default regularization parameters, and does not require parameter tuning which can make it easy
188 to apply from a users's point of view.

189 We compared Loter to other local ancestry software packages HAPMIX, RFMIX, and LAMP-LD. We found that
190 the diploid accuracy obtained with HAPMIX is reduced by 32% in average when haplotypes are not known perfectly
191 using trio-phasing but only reconstructed using phasing software such as Beagle. By contrast, RFMIX, LAMP-LD,
192 and Loter are robust to imperfect haplotype reconstruction and that is the reason why only RFMIX, LAMP-LD, and
193 Loter were further considered in software comparisons. When admixture took place 5 generations ago, RFMIX and
194 LAMP-LD provide the largest diploid accuracies but all three software were found to provide an accurate reconstruc-
195 tion of local ancestry with diploid accuracies always larger than 99% for the simulations of Afro-American admixed
196 haplotypes and larger than 89.9% for the simulations of Populus individuals. Compared to RFMIX and LAMP-LD,
197 results obtained with Loter are more robust with respect to the time since admixture occurred. For simulated human
198 data, the diploid accuracy of Loter decreases to 87% for the most ancient admixture times of 500 generations whereas
199 it decreases to 72% and 81% when using RFMIX and LAMP-LD. For Populus data, diploid accuracy does not depend
200 on admixture times when using Loter and LAMP-LD whereas it is severely impacted when using RFMIX. The fact
201 that diploid accuracy is not impacted by the considered range of admixture times is encouraging and suggests that
202 local ancestry inference is possible for admixture that occurred hundreds of generation ago when SNP density is large
203 enough, as for Populus data; the mean distance between two SNPs being of $9.8 \cdot 10^{-6}$ cM for Populus data and of
204 $2.7 \cdot 10^{-3}$ cM for the human data.

205 The reason why diploid accuracy may be impacted by admixture time is related to the statistical smoothing proce-
206 dure. For instance, RFMIX has been tuned to genotypes resulting from recent admixture that occurred 10 generations
207 ago or less such as admixture between African and Europeans (Gravel 2012; Bryc et al. 2015). When using default
208 parameters of RFMIX for data resulting from ancient admixture events, reconstructed ancestry tracts are inadequately
209 long (Figure 5 and Supplementary Figure SI6) and over-smoothing can affect diploid accuracy. Even when provid-
210 ing true admixture time to RFMIX, diploid accuracy of RFMIX remains more impacted by admixture time possibly

211 because of the default of 0.2 cM for window size (Supplementary Figure SI7). When using HAPMIX, a choice of
 212 window lengths or of the time since admixture should also be provided. However, choice of admixture time can be
 213 very difficult to estimate and impacts biological results. For instance, lengths of ancestry tracts found with HAPMIX
 214 depend on the input value for admixture time (Patin et al. 2014). The model averaging procedure implemented in Loter
 215 has the advantage to avoid to put a strong prior on a particular length of ancestry tract. In addition, model averaging
 216 improves parameter inference, which has already been observed when phasing genotypes using a statistical model of
 217 Linkage Disequilibrium (Scheet and Stephens 2006).

218 The simulation results show that accuracy obtained with Loter and LAMP-LD is less sensitive to admixture times
 219 compared to the accuracy obtained with RFMix. LAMP-LD is more accurate than Loter for recent admixture times
 220 when using human data and for all values of admixture times when considering the Populus data. However, LAMP-LD
 221 has limitations for large-scale NGS data that contains a large number of molecular markers. It is limited to run on
 222 50,000 SNPs and it can be computer intensive. To perform local ancestry inference for 500,000 SNPs and 20 admixed
 223 Populus individuals, the running time is of 28 minutes using RFMIX, 58 minutes with LAMP-LD and of 6 minutes
 224 using LAMP-LD when using 20 Intel Xeon processors of 2.40 GhZ. However, although there are differences between
 225 LAI software packages, using different LAI software packages can be a wise strategy to provide enhanced evidence for
 226 an association or a selection signal (Zhou et al. 2016). We expect that providing a parameter-free and rapid software
 227 for local ancestry inference will make more accessible genomic studies about admixture processes.

228 **Materials and Methods**

229 **Dynamic Programming**

230 The optimization problem of equation (1) is solved using dynamic programming. The solution of the problem with
 231 p SNPs can be derived from the solution with $(p - 1)$ SNPs. Two configurations are possible. Either the admixed
 232 haplotype copies from the same haplotype at the $(p - 1)^{\text{th}}$ and p^{th} SNP and

$$C(s_1, \dots, s_p) = C(s_1, \dots, s_{p-1}) + |h^p - H_{s_{p-1}}^p|, \quad (2)$$

233 or it uses different template haplotypes and

$$C(s_1, \dots, s_p) = C(s_1, \dots, s_{p-1}) + |h^p - H_{s_p}^p| + \lambda. \quad (3)$$

234 The optimal solution is then found by computing the shortest path on a graph displayed in Supplementary Figure
 235 SI5. To find the shortest path, dynamic programming computes at each node a quantity $Q(i, j)$ that corresponds to

236 the optimal solution for the first j SNPs and when the template haplotype at SNP j is the i^{th} haplotype $s_j = i$. The
 237 quantity $Q(i, j)$ is updated as followed

$$Q(i, j) = \min \left(Q(i, j-1), \min_{i' \in \{1, \dots, n\}} \{Q(i', j-1)\} + \lambda \right) + |h^j - H_i^j| \quad (4)$$

238 Because we store the value of $\min_{i' \in \{1, \dots, n\}} \{Q(i', j-1)\}$ at locus $j-1$, the value of $Q(i, j)$ can be computed
 239 as a minimum between 2 values. For each admixed haplotype, the complexity of this algorithm is therefore $\mathcal{O}(n \times p)$
 240 where n is the number of individuals in the ancestral populations and p is the number of SNPs. The path (s_1, \dots, s_p)
 241 is then converted to an haploid ancestry sequence $a = (a_1, \dots, a_p) \in (1, \dots, K)^p$ where a_j is the population of origin
 242 of the s_j^{th} haplotype.

243 Accounting for phase errors of admixed genotypes

244 Reconstructed haplotypes from an admixed population may contain switch errors (Browning and Browning 2011). As
 245 considered in RFMix, it is possible to redistribute ancestry chunks among the two haplotypes from the same individual
 246 in order to correct for switch errors. For now, the software Loter accounts for phase error when there are 2 ancestral
 247 populations only. Once local ancestry values for each of the 2 haplotypes have been found after solving equation (1),
 248 we compute the sum of the 2 haplotypic local ancestries resulting in diploid local ancestry values $d = (d^1, \dots, d^p) \in$
 249 $\{0, 1, 2\}^p$ as returned by the software HAPMIX. Local ancestry values are then reconstructed using an internal *ancestry*
 250 *phasing* algorithm. The phasing procedure considers that the 2 haplotypic local ancestry sequences are a mosaic of
 251 two possible ancestry sequences $A_1 = (0, \dots, 0)$ and $A_2 = (1, \dots, 1)$ corresponding to the two possible ancestral
 252 populations. Two vectors $(s_1, \dots, s_p) \in \{0, 1\}^p$ and $(s'_1, \dots, s'_p) \in \{0, 1\}^p$ describe the sequence of labels, two
 253 vectors $a \in \{0, 1\}^p$ and $a' \in \{0, 1\}^p$ are the haploid local ancestry values, and Θ is a compound parameter equal to
 254 $(s_1, \dots, s_p, s'_1, \dots, s'_p, a, a')$. The ancestry phasing algorithm consists of minimizing the following cost function

$$C'(\Theta) = \sum_{j=1}^p |a^j - A_{s_j}^j| + \sum_{j=1}^p |a'^j - A_{s'_j}^j| + \lambda \sum_{j=1}^{p-1} \mathbb{1}_{s_j \neq s_{j+1}} + \lambda \sum_{j=1}^{p-1} \mathbb{1}_{s'_j \neq s'_{j+1}}, \quad (5)$$

255 subject to the constraint that the sum of the haploid local ancestries a and a' is equal to the diploid local ancestry d . The
 256 solution for Θ is found using dynamic programming. For each admixed individual, the complexity of this algorithm is
 257 $\mathcal{O}(p)$. Once a solution has been found, haplotypic local ancestry, which has been corrected for phasing errors, consists
 258 of the two sequences $(A_{s_1}^1, \dots, A_{s_p}^p)$ and $(A_{s'_1}^1, \dots, A_{s'_p}^p)$.

259 **Admixture between Populus species**

260 We simulate admixed individuals by constructing their genomes from a mosaic of real *P. balsamifera* and *P. trichocarpa*
261 individuals (Suarez-Gonzalez et al. 2016). We consider a probabilistic model that has already been used to simulate
262 admixed individuals and to evaluate the performances of HAPMIX (Price et al. 2009). Simulations are based on 20
263 haplotypes (first 50,000 SNPs) from chromosome 6 from the species *P. balsamifera* (balsam poplar) and of 20 hap-
264 lotypes from the species *P. trichocarpa* (black cottonwood) (Suarez-Gonzalez et al. 2016). Haplotypes were obtained
265 from genotypes using Beagle (Browning and Browning 2007). The *P. trichocarpa* ancestry α_i of a simulated admixed
266 individual is drawn randomly according to a Beta distribution of mean 0.8 and of variance 0.1. At the first marker, the
267 haplotype of an admixed individual i is assumed to originate from *P. trichocarpa* with a probability α_i and from *P. bal-*
268 *samifera* otherwise. For each simulated haplotype, we associate one *P. balsamifera* haplotype and one *P. trichocarpa*
269 haplotype. For a given admixed individual, haplotypes are exclusively copied from these two source haplotypes that
270 are chosen at random. The length (measured in Morgans) of an ancestry chunk is drawn according to an exponential
271 distribution of rate μ generations. In the simulations, we consider values for μ ranging from 5 to 500 generations.
272 The species origin of the new ancestry tract is again determined using the $(\alpha_i, 1 - \alpha_i)$ admixture coefficients and the
273 copying process for haplotype is repeated as before. To reconstruct local ancestry of simulated admixed individuals, we
274 consider 30 haplotypes from *P. balsamifera* and 30 haplotypes from *P. trichocarpa* that were not used when simulating
275 admixed individuals. Haplotypes were again phased using the software Beagle. To evaluate diploid accuracy for a
276 given value of μ , we consider 20 sets of simulations consisting of 20 admixed haplotypes each.

277 **Admixture between human populations**

278 When simulating admixed individuals between Yorubans (YRI) and Europeans (CEU) from HAPMAP 3, we consider
279 the copying process mentioned before. For simulations, we consider true haplotypes based on trio phasing. For infer-
280 ence, we consider haplotypes reconstructed using Beagle based on genotypes that are not used for simulations. A total
281 of 48 Yoruban haplotypes and of 48 European haplotypes are considered to simulate 48 Afro-American haplotypes.
282 We consider 40 European haplotypes and 40 African haplotypes, which were obtained with Beagle, to perform local
283 ancestry inference. To evaluate diploid accuracy for a given value of μ , we consider 20 sets of simulations consisting
284 of 48 admixed haplotypes each.

285 We consider an additional set of simulations where 3 populations admixed. Admixture is assumed to occur be-
286 tween Chinese (CHB), Europeans (CEU) and Africans (YRI). The exponential distribution for European chunks is
287 of rate $\mu \in \{5, 100, 200, 500\}$ generations and the exponential distribution for African and Asian chunks is equal to
288 $\mu/2$ generations. By contrast to the 2-way admixture models, we use trio-phased haplotypes for inference and not
289 haplotypes reconstructed with Beagle.

290 **Admixed Populus individuals**

291 We consider 36 individuals that are admixed between *P. balsamifera* and *P. trichocarpa* (Suarez-Gonzalez et al. 2016)
292 and use Beagle to phase them. We use the first 500,000 SNPs of chromosome 6 to reconstruct ancestry tracts. We
293 simulate 16 admixed individuals based on 20 genotypes from *P. balsamifera* and *P. trichocarpa* species. Instead of
294 considering true ancestry ancestry tracts, we rather replicate the same pipeline as for real data such as the bias of
295 ancestry tract reconstruction should be same for data and simulations. We phase simulated individuals using Beagle
296 and reconstruct ancestry tracts using Loter.

297 **Software**

298 The Loter software package and its source code are available at <https://github.com/bcm-uga/Loter>.

299 **Data**

300 Human HapMap 3 data are available online at <http://www.sanger.ac.uk/resources/downloads/human/hapmap3.html>. Populus data are available online at <http://datadryad.org/resource/doi:10.5061/dryad.0817m>.

303 **Acknowledgments**

304 Authors acknowledge Grenoble Alpes Data Institute, supported by the French National Research Agency under the
305 “Investissements d’avenir” program (ANR-15-IDEX-02), the LabEx PERSYVAL-Lab (ANR-11-LABX-0025-01) and
306 the MACARON project (ANR-14-CE23-0003-01). JM is also supported by a grant from the European Research
307 Council (SOLARIS project, number 714381).

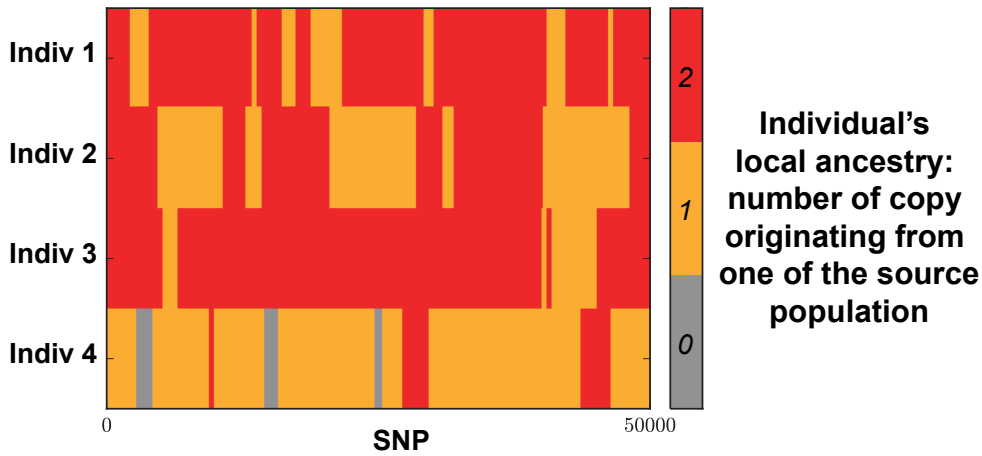


Figure 1: Example of local ancestry inference for 4 simulated *Populus* individuals resulting from admixture between 2 *Populus* species, which are *Populus trichocarpa* and *Populus balsamifera* (Suarez-Gonzalez et al. 2016). For an admixed individual, local ancestry at a given locus corresponds to the number of copies that has been inherited from the species *P. trichocarpa*. LAI software require haplotypes from putative source populations and process haplotypes or genotypes from admixed population to return local ancestry of admixed individuals. Details of the simulations are described in the Materials and Methods section.

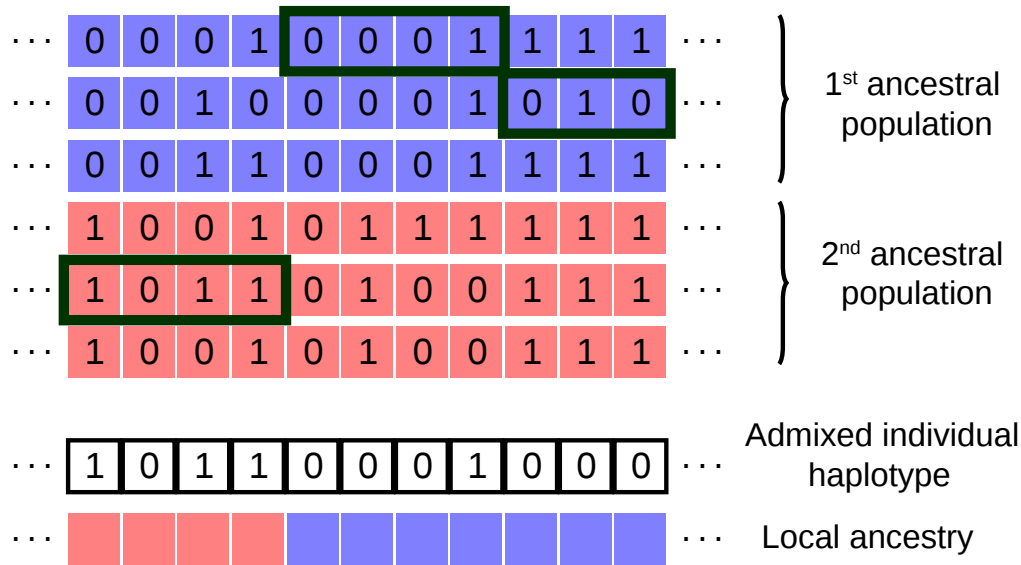


Figure 2: Graphical description of Local Ancestry Inference as implemented in the software Loter. Given a collection of parental haplotypes from the source populations depicted in blue and red, Loter assumes that an haplotype of an admixed individuals is modeled as a mosaic of existing parental haplotypes. In this example, the 1st term of equation (1) (loss function) is equal to 1 because of a single mismatch between parental and admixed haplotype located at the next-to-last position, and the 2nd term of equation (1) (regularization term) is equal to 2λ because there are 2 switches between parental haplotypes. The displayed solution corresponds to the mathematical solution $(s_1, \dots, s_{11}) = (5, 5, 5, 5, 1, 1, 1, 1, 2, 2, 2)$ where haplotypes are numbered from top to bottom, and $s_j = k$ if the admixed haplotype results from a copy of the k^{th} parental haplotype at the j^{th} SNP.

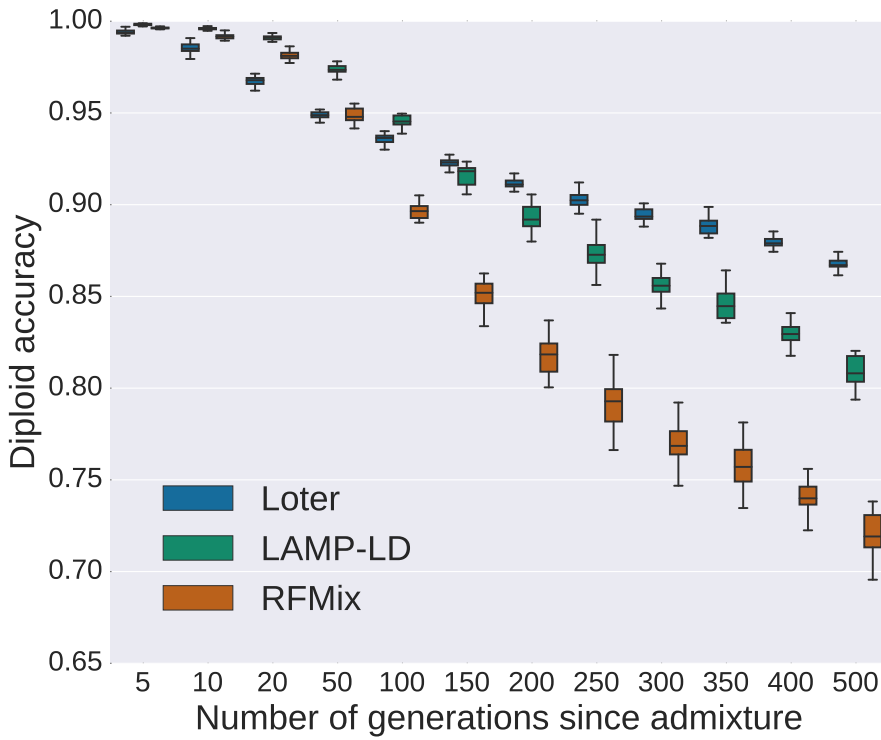


Figure 3: Diploid accuracy obtained with LAMP-LD, Loter, and RFMix for simulated admixed human individuals as a function of the time since admixture occurred. Admixed individuals are simulated by constructing their genomes from a mosaic of true African (YRI) and European (CEU) haplotypes (International HapMap 3 Consortium et al. 2010). For performing simulations, true haplotypes are obtained using trio information. For local ancestry inference, haplotypes are obtained with Beagle using individuals that are not used for simulating admixed individuals. For each value of the number of generations since admixture, 20 sets of 48 admixed individuals are generated. Boxplots show the distribution of the 20 values for the mean diploid accuracy.

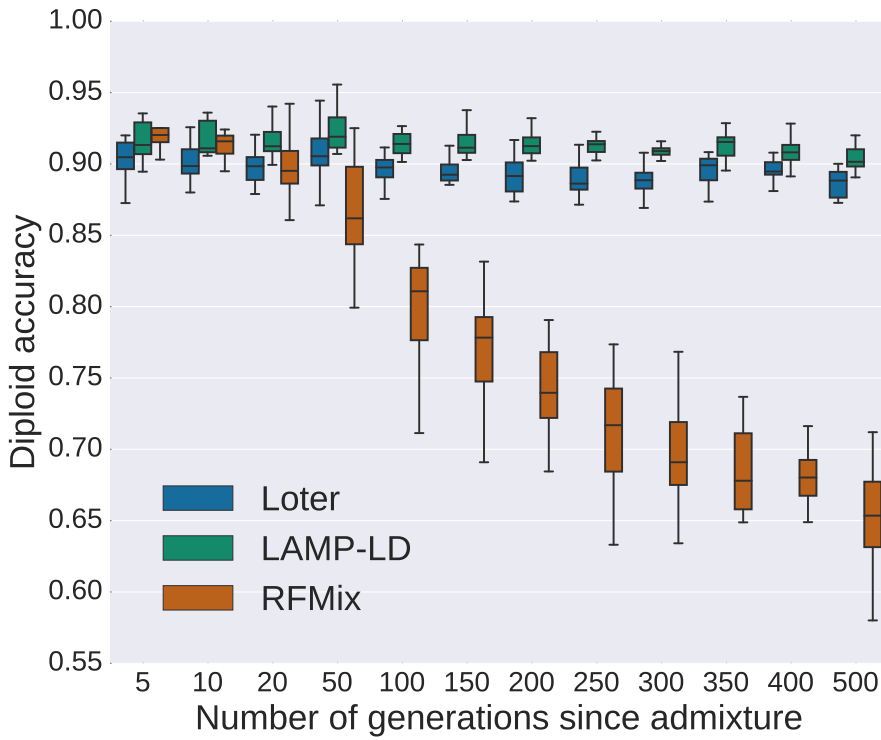


Figure 4: Diploid accuracy obtained with LAMP-LD, Loter, and RFMix for simulated admixed *Populus* individuals as a function of the time since admixture occurred. Admixed individuals are simulated by constructing their genomes from a mosaic of *Populus trichocarpa* and *Populus balsamifera* individuals. Individuals are phased using Beagle and two different sets of individuals are used for performing simulations and inference. For each value of the number of generations since admixture, 20 sets of 20 admixed individuals are generated. Boxplots show the distribution of the 20 values for the mean diploid accuracy.

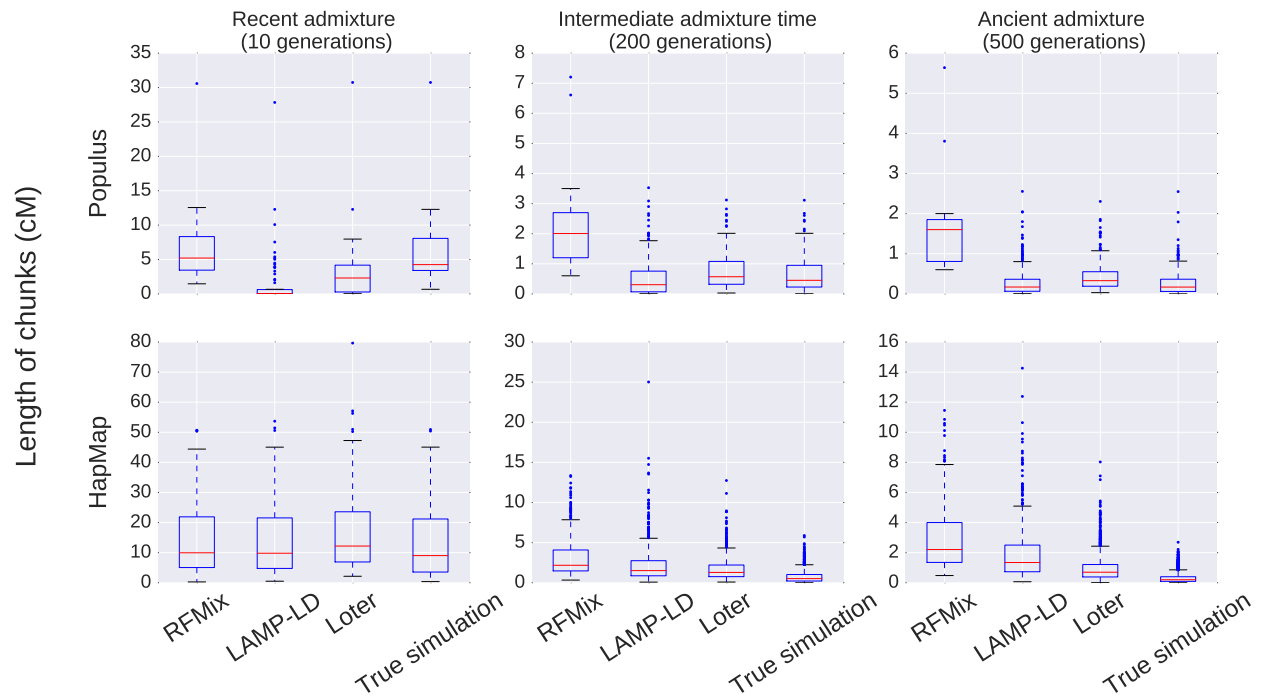


Figure 5: Distribution of the length of ancestry chunks for simulated data. For Populus data, we consider the first 500,000 SNPs of chromosome 6 and for human data, we consider the first 50,000 SNPs of chromosome 1. When considering Populus data, we run 10 times LAMP-LD on non-overlapping sets of SNPs in order to avoid the limitation of 50,000 SNPs of LAMP-LD.

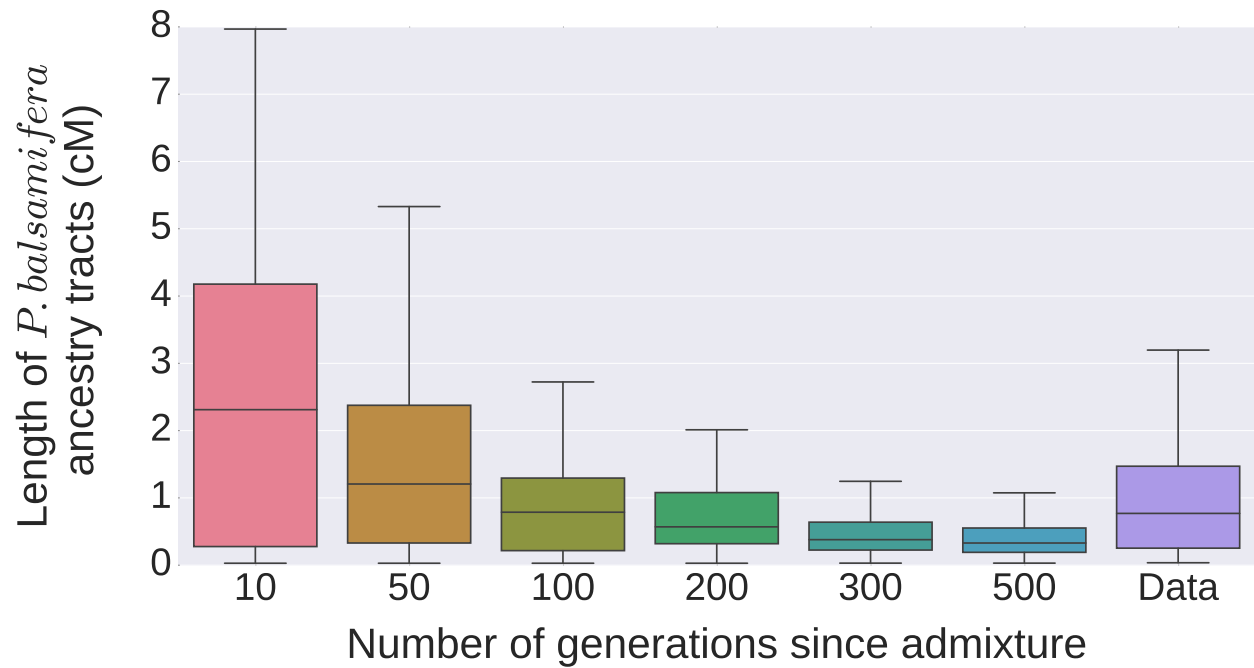


Figure 6: Distribution of the length of *P. balsamifera* ancestry tracts. The data consist of genotypes of admixed individuals between *P. balsamifera* and *P. trichocarpa*. For the simulations, we replicate the same pipeline as for local inference with real data, which consist of using Beagle to phase genotypes and Loter to reconstruct ancestry tracts.

	HAPMIX	LAMP-LD	RFMix	Loter
Phasing of admixed individuals	No	No	Yes	Yes
Number of ancestral pop.	2	2, 3, 5	≥ 2	≥ 2
Genetic map required (in cM)	Yes	No (Physical position)	Yes	No (Ordered SNPs)
Limitation of the number of SNPS	No	50,000	No	No
Phasing error correction	No	Not required	Yes	Yes for 2 ancestral pop.
Parallel implementation	No	No	Yes	Yes
Admixture time required	Yes	No	Yes	No
Other biological param. required	Yes	No	No	No

Table 1: Differences between several LAI software. The abbreviation param. stands for parameter and pop. for population. Other biological parameters required by HAPMIX are recombination and mutation rates.

References

- Baran, Y., Pasaniuc, B., Sankararaman, S., Torgerson, D. G., Gignoux, C., Eng, C., Rodriguez-Cintron, W., Chapela, R., Ford, J. G., Avila, P. C. et al. 2012. Fast and accurate inference of local ancestry in Latino populations. *Bioinformatics* **28**:1359–1367.
- Brandvain, Y., Kenney, A. M., Flagel, L., Coop, G. and Sweigart, A. L. 2014. Speciation and Introgression between *mimulus nasutus* and *mimulus guttatus*. *PLoS Genet* **10**:e1004410.
- Breiman, L. 1996. Bagging predictors. *Machine learning* **24**:123–140.
- Browning, S. R. and Browning, B. L. 2007. Rapid and accurate haplotype phasing and missing-data inference for whole-genome association studies by use of localized haplotype clustering. *The American Journal of Human Genetics* **81**:1084–1097.
- . 2011. Haplotype phasing: existing methods and new developments. *Nature Reviews Genetics* **12**:703–714.
- Bryc, K., Durand, E., Macpherson, J. M., Reich, D. and Mountain, J. 2015. The genetic ancestry of African, Latino, and European Americans across the United States. *American Journal of Human Genetics* **96**:37–53.
- Buerkle, C. A. and Lexer, C. 2008. Admixture as the basis for genetic mapping. *Trends in ecology & evolution* **23**:686–694.
- Corbett-Detig, R. and Nielsen, R. 2017. A hidden Markov model approach for simultaneously estimating local ancestry and admixture time using next generation sequence data in samples of arbitrary ploidy. *PLoS genetics* **13**:e1006529.
- Gravel, S. 2012. Population genetics models of local ancestry. *Genetics* **191**:607–619.
- Hufford, M. B., Lubinsky, P., Pyhäjärvi, T., Devengenzo, M. T., Ellstrand, N. C. and Ross-Ibarra, J. 2013. The genomic signature of crop-wild introgression in maize. *PLoS Genet* **9**:e1003477.

328 International HapMap 3 Consortium et al. 2010. Integrating common and rare genetic variation in diverse human
329 populations. *Nature* **467**:52–58.

330 Li, N. and Stephens, M. 2003. Modeling linkage disequilibrium and identifying recombination hotspots using single-
331 nucleotide polymorphism data. *Genetics* **165**:2213–2233.

332 Lindtke, D., Gonzalez-Martinez, S., Macaya-Sanz, D. and Lexer, C. 2013. Admixture mapping of quantitative traits in
333 *Populus* hybrid zones: power and limitations. *Heredity* **111**:474–485.

334 Liu, S., Lorenzen, E. D., Fumagalli, M., Li, B., Harris, K., Xiong, Z., Zhou, L., Korneliussen, T. S., Somel, M., Babbitt,
335 C. et al. 2014. Population genomics reveal recent speciation and rapid evolutionary adaptation in polar bears. *Cell*
336 **157**:785–794.

337 Maples, B. K., Gravel, S., Kenny, E. E. and Bustamante, C. D. 2013. RFMix: a discriminative modeling approach for
338 rapid and robust local-ancestry inference. *The American Journal of Human Genetics* **93**:278–288.

339 Medugorac, I., Graf, A., Grohs, C., Rothhammer, S., Zagdsuren, Y., Gladyr, E., Zinovieva, N., Barbieri, J., Seichter, D.,
340 Russ, I. et al. 2017. Whole-genome analysis of introgressive hybridization and characterization of the bovine legacy
341 of Mongolian yaks. *Nature Genetics* **49**:470–475.

342 Ni, X., Yang, X., Guo, W., Yuan, K., Zhou, Y., Ma, Z. and Xu, S. 2016. Length distribution of ancestral tracks under a
343 general admixture model and its applications in population history inference. *Scientific reports* **6**.

344 Patin, E., Siddle, K. J., Laval, G., Quach, H., Harmant, C., Becker, N., Froment, A., Régnault, B., Lemée, L., Gravel,
345 S. et al. 2014. The impact of agricultural emergence on the genetic history of african rainforest hunter-gatherers and
346 agriculturalists. *Nature communications* **5**:3163.

347 Patterson, N., Hattangadi, N., Lane, B., Lohmueller, K. E., Hafler, D. A., Oksenberg, J. R., Hauser, S. L., Smith,
348 M. W., O'Brien, S. J., Altshuler, D. et al. 2004. Methods for high-density admixture mapping of disease genes. *The*
349 *American Journal of Human Genetics* **74**:979–1000.

350 Payseur, B. A. and Rieseberg, L. H. 2016. A genomic perspective on hybridization and speciation. *Molecular ecology*
351 **25**:2337–2360.

352 Price, A. L., Tandon, A., Patterson, N., Barnes, K. C., Rafaels, N., Ruczinski, I., Beaty, T. H., Mathias, R., Reich,
353 D. and Myers, S. 2009. Sensitive detection of chromosomal segments of distinct ancestry in admixed populations.
354 *PLoS Genet* **5**:e1000519.

355 Sankararaman, S., Sridhar, S., Kimmel, G. and Halperin, E. 2008. Estimating local ancestry in admixed populations.
356 *The American Journal of Human Genetics* **82**:290–303.

- 357 Scheet, P. and Stephens, M. 2006. A fast and flexible statistical model for large-scale population genotype data:
358 applications to inferring missing genotypes and haplotypic phase. *The American Journal of Human Genetics* **78**:629–
359 644.
- 360 Seldin, M. F., Pasaniuc, B. and Price, A. L. 2011. New approaches to disease mapping in admixed populations. *Nature*
361 *Reviews Genetics* **12**:523–528.
- 362 Suarez-Gonzalez, A., Hefer, C. A., Christe, C., Corea, O., Lexer, C., Cronk, Q. C. and Douglas, C. J. 2016. Genomic
363 and functional approaches reveal a case of adaptive introgression from *populus balsamifera* (balsam poplar) in *p.*
364 *trichocarpa* (black cottonwood). *Molecular ecology* **25**:2427–2442.
- 365 vonHoldt, B. M., Kays, R., Pollinger, J. P. and Wayne, R. K. 2016. Admixture mapping identifies introgressed genomic
366 regions in North American canids. *Molecular ecology* **25**:2443–2453.
- 367 Xue, J., Lencz, T., Darvasi, A., Pe'er, I. and Carmi, S. 2017. The time and place of european admixture in Ashkenazi
368 Jewish history. *PLoS genetics* **13**:e1006644.
- 369 Zhou, Q., Zhao, L. and Guan, Y. 2016. Strong selection at MHC in Mexicans since admixture. *PLoS genetics*
370 **12**:e1005847.

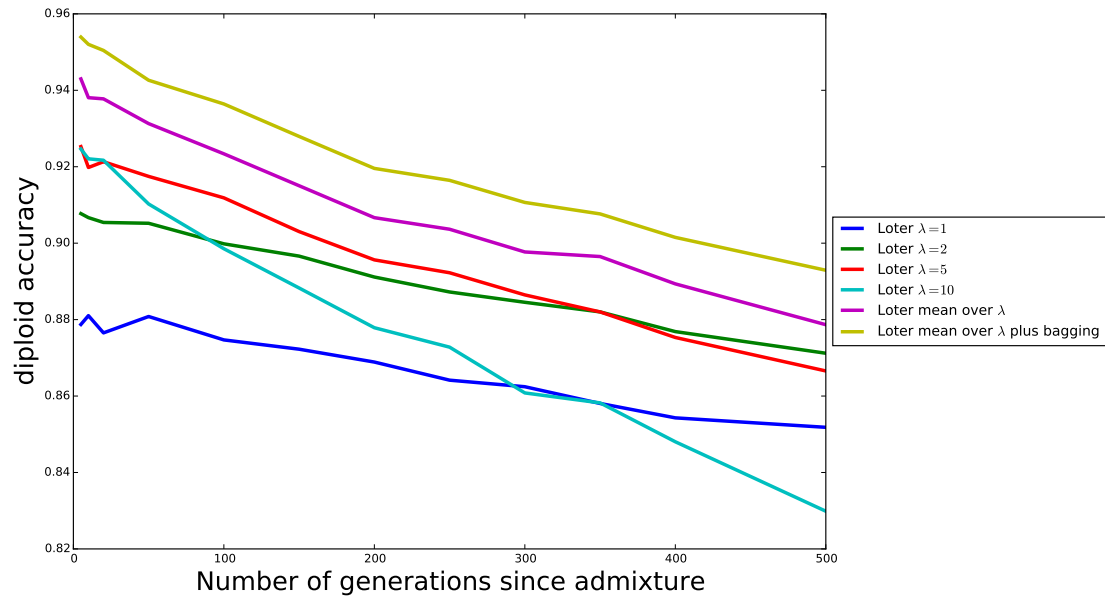


Figure SI1: Diploid accuracy obtained with Loter is improved when bagging and when averaging over multiple values of the regularization parameter. Admixed individuals were simulated by constructing their genomes from a mosaic of true African (YRI) and European (CEU) haplotypes (International HapMap 3 Consortium et al. 2010) (Figure 3). Diploid accuracies are evaluated for twelve different values of the admixture time corresponding to 5, 10, 20, 50, 100, 150, 200, 250, 300, 350, 400 and 500 generations.

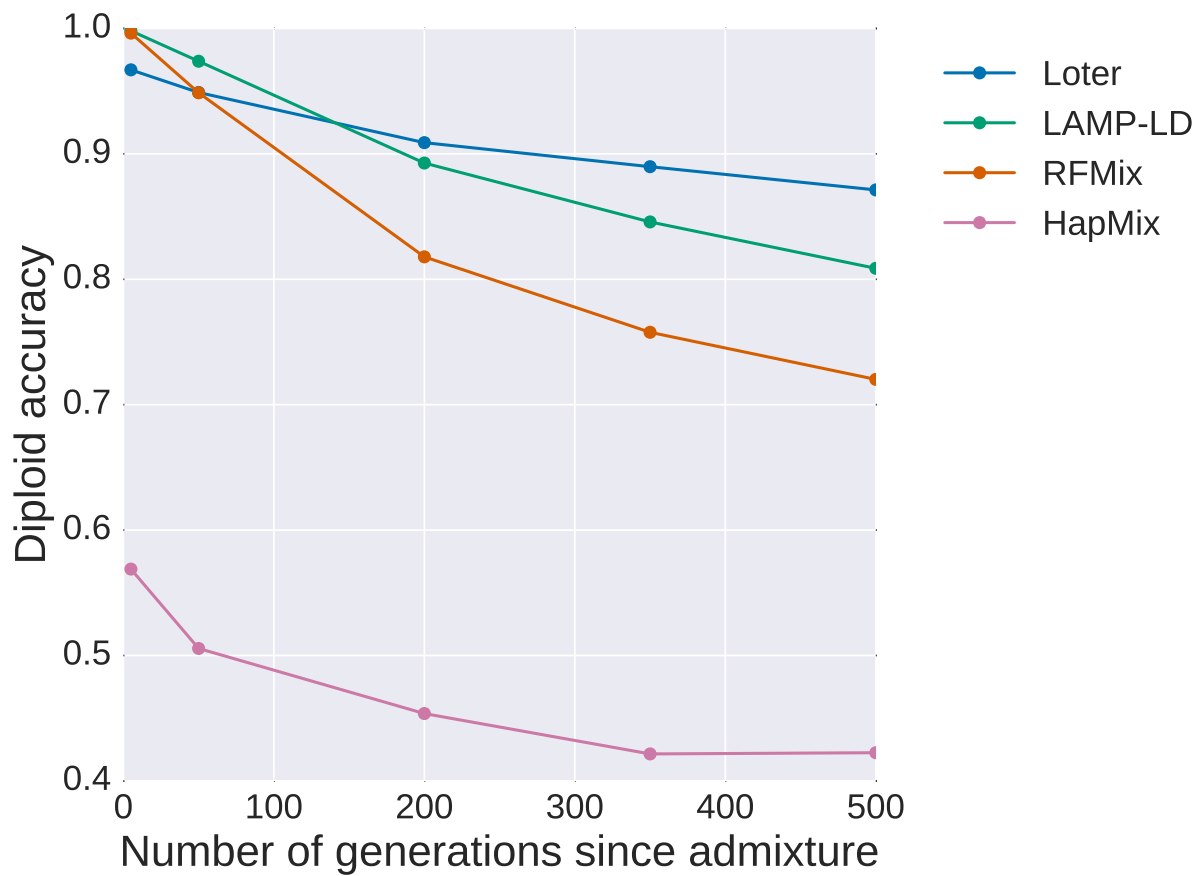


Figure SI2: Diploid accuracy obtained with LAMP-LD, Loter, and RFMix for simulated human individuals as a function of the time since admixture occurred. Admixed individuals are simulated by constructing their genomes from a mosaic of true African (YRI) and European (CEU) haplotypes (International HapMap 3 Consortium et al. 2010) (Figure 3). For each admixture time, HAPMIX is evaluated using a single simulation of 48 admixed individuals. Other software, which run faster, are evaluated based on the mean diploid accuracy obtained with 20 simulated sets of 48 admixed individuals.

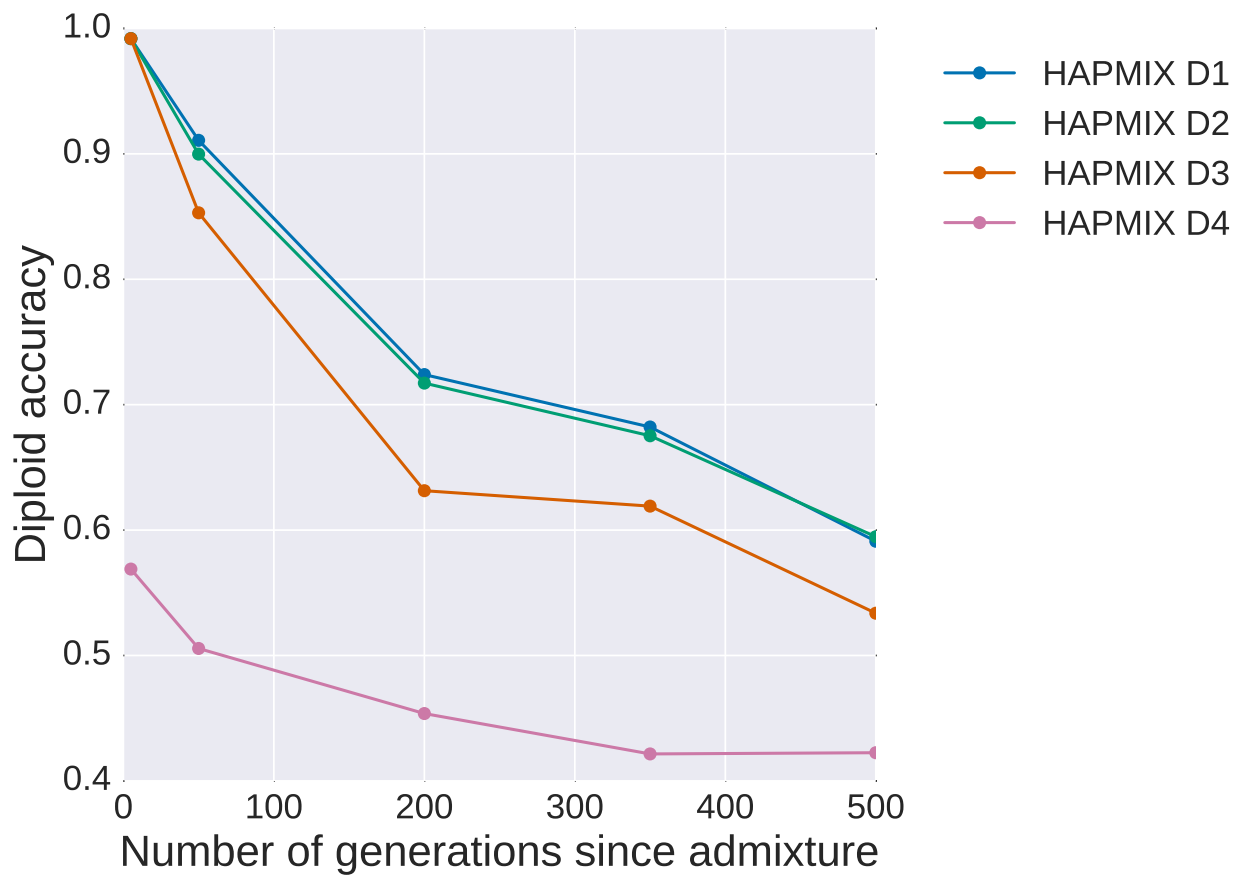


Figure SI3: Diploid accuracy obtained with HAPMIX using four different haplotype sets for LAI. The diploid accuracy of HAPMIX is severely reduced when considering reconstructed haplotypes of admixed individuals instead of true haplotypes. Admixed individuals are simulated by constructing their genomes from a mosaic of true African (YRI) and European (CEU) haplotypes (International HapMap 3 Consortium et al. 2010) (Figure 3). In set D1, we consider the same true haplotypes (trio-phased) for simulations and inference. In set D2, we consider different haplotypes for simulations and inference but haplotypes are all trio-phased and admixture time is assumed to be known. The set D3 is the same as D2 except that admixture time is unknown and assume to be equal to 6 generations. In set D4, haplotypes used for inference are not true haplotypes but have been reconstructed with Beagle.

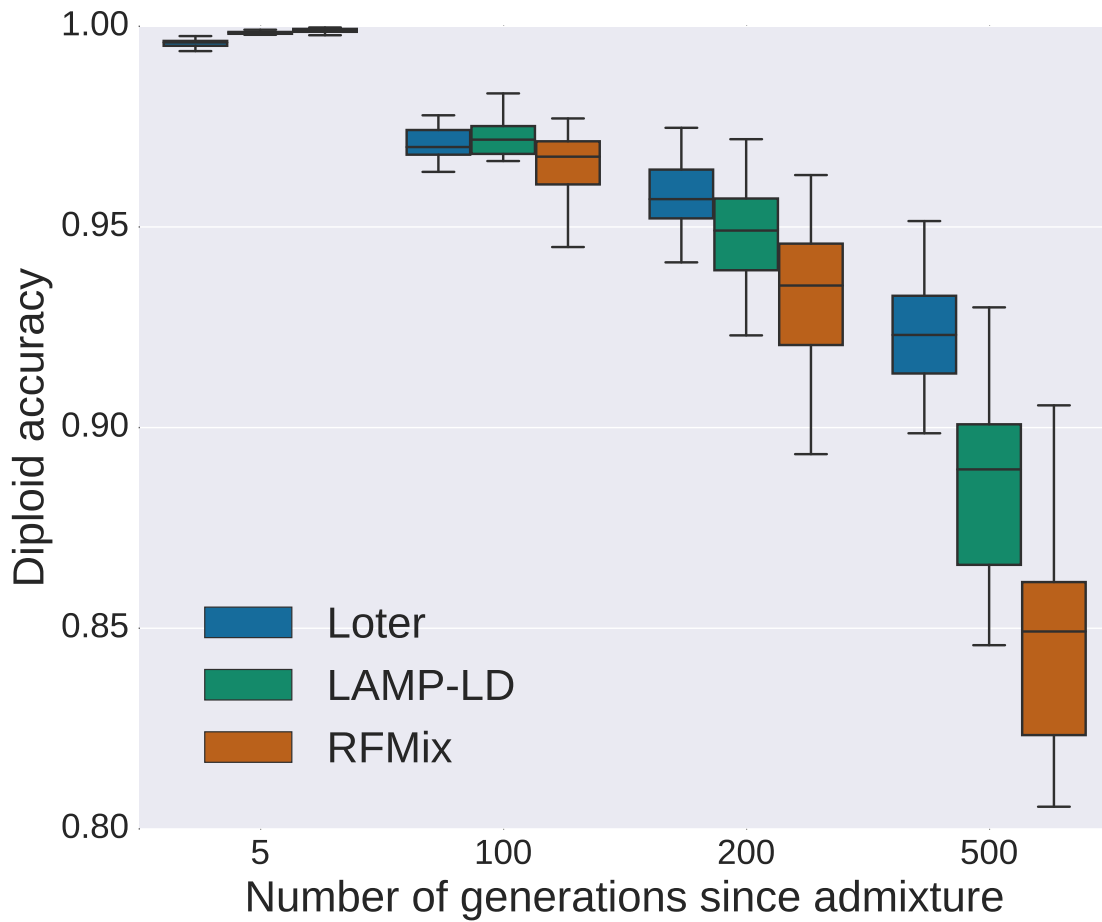


Figure SI4: Diploid accuracy obtained under a 3-way admixture model with LAMP-LD, Loter, and RFMix for simulated admixed human individuals as a function of the time since admixture occurred. Admixed individuals are simulated by constructing their genomes from a mosaic of true African (YRI), European (CEU), and Chinese haplotypes (International HapMap 3 Consortium et al. 2010). For performing simulations, true haplotypes are obtained using trio information. For local ancestry inference, haplotypes are also reconstructed using trio-based inference and are different from haplotypes used for simulations. For each value of the number of generations since admixture, 20 sets of 20 admixed individuals are generated. Boxplots show the distribution of the 20 values for the mean diploid accuracy.

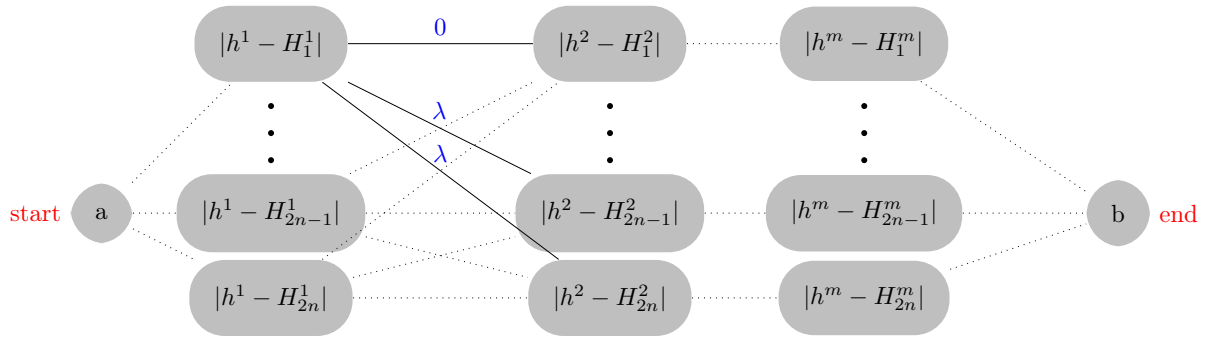


Figure S15: Graph that represents the optimization problem of equation (1). An optimal solution for (s_1, \dots, s_p) is found by finding the shortest path from node a to node b .

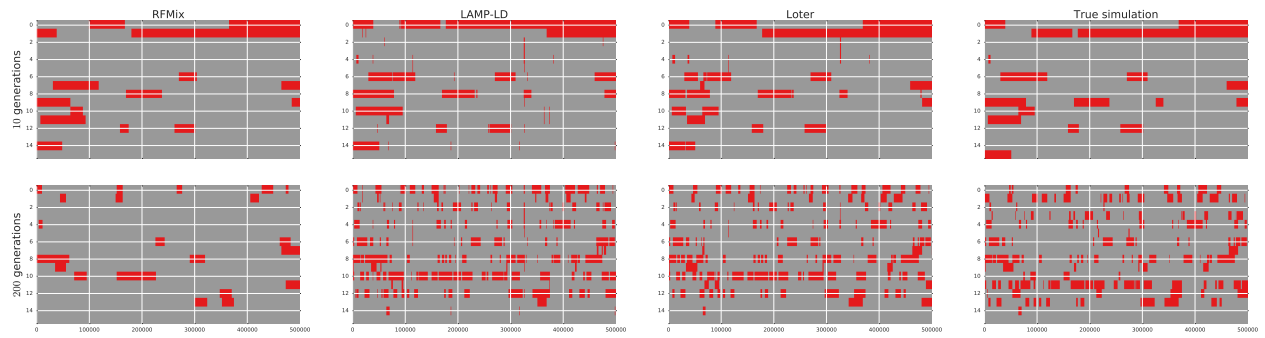


Figure SI6: Ancestry tracts for 20 simulated admixed *Populus* individuals. Grey chunks correspond to *P. trichocarpa* chunks and red chunks correspond to *P. balsamifera* chunks. Two rows correspond to the two haplotypes of a single individual. Ancestry switches between haplotypes are caused by haplotype phasing using Beagle. The presence of spurious and small ancestry chunks contribute to excessively decrease the median length of ancestry chunks in LAMP-LD and Loter.

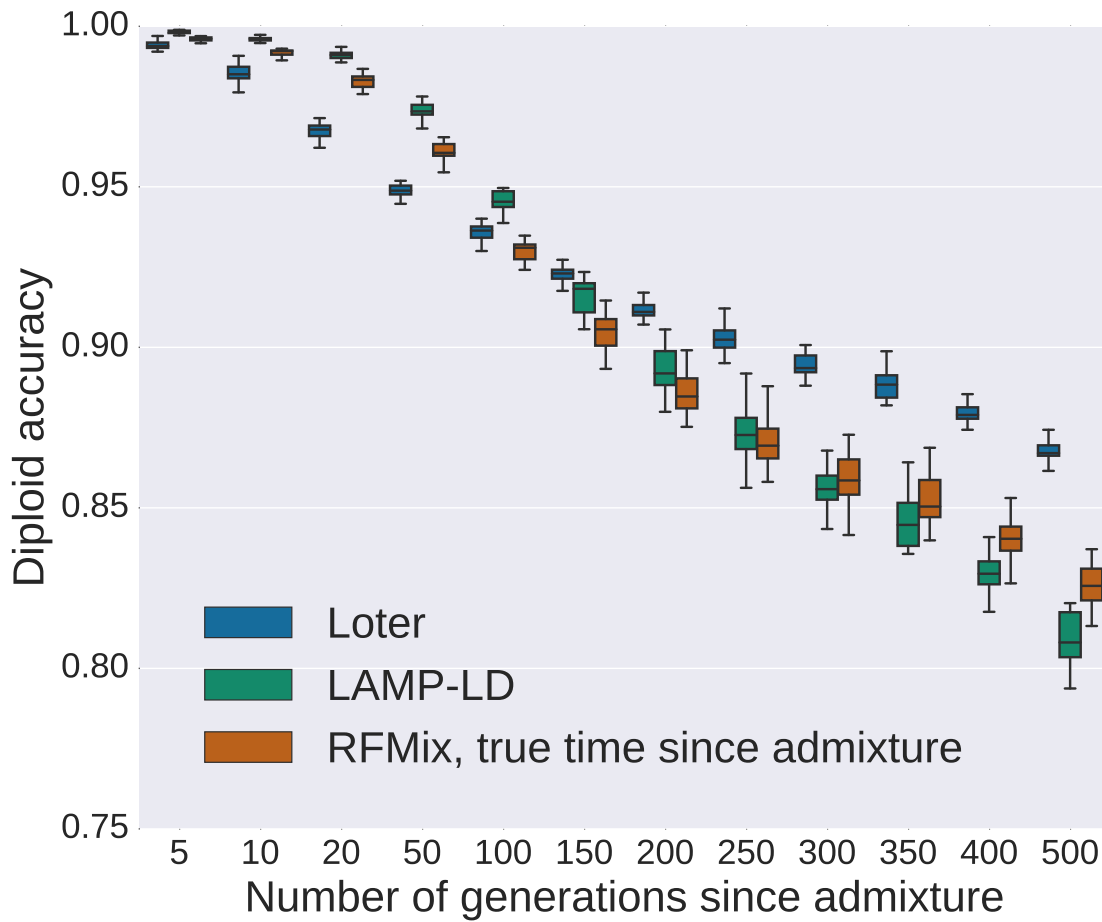


Figure SI7: Diploid accuracy obtained with LAMP-LD, Loter, and RFMix for simulated admixed *Populus* individuals as a function of the time since admixture occurred when true values of the time since admixture are provided to RFMIX. Admixed individuals are simulated by constructing their genomes from a mosaic of *Populus trichocarpa* and *Populus balsamifera* individuals. Individuals are phased using Beagle and two different sets of individuals are used for performing simulations and inference. For each value of the number of generations since admixture, 20 sets of 20 admixed individuals are generated. Boxplots show the distribution of the 20 values for the mean diploid accuracy.